PASSAGE OF PARTICLES THROUGH MATTER

To reduce the size of this section's PostScript file, we have divided it into three PostScript files. We present the following index:

PART 1

PART 2

PART 3

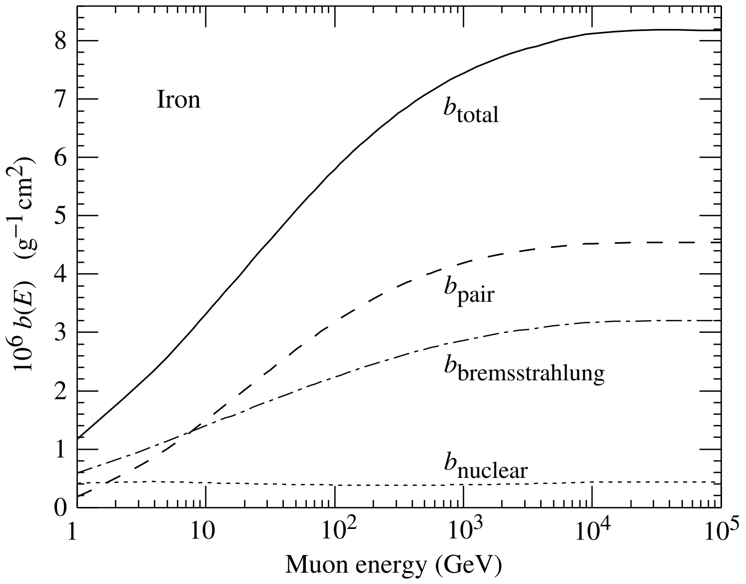

Figure 23.10: Contributions to the fractional energy loss by muons in iron due to e^+e^- pair production, bremsstrahlung, and photonuclear interactions, as obtained from Lohmann *et al.* [44].

23.6. Muon energy loss at high energy

At sufficiently high energies, radiative processes become more important than ionization for all charged particles. For muons and pions in materials such as iron, this "critical energy" occurs at several hundred GeV. Radiative effects dominate the energy loss of energetic muons found in cosmic rays or produced at the newest accelerators. These processes are characterized by small cross sections, hard spectra, large energy fluctuations, and the associated generation of electromagnetic and (in the case of photonuclear interactions) hadronic showers [45–53]. As a consequence, at these energies the treatment of energy loss as a uniform and continuous process is for many purposes inadequate.

It is convenient to write the average rate of muon energy loss as [43]

$$-dE/dx = a(E) + b(E)\,E\ . \tag{23.28}$$

Here $a(E)$ is the ionization energy loss given by Eq. (23.1), and $b(E)$ is the sum of e^+e^- pair production, bremsstrahlung, and photonuclear contributions. To the approximation that these slowly-varying functions are constant, the mean range x_0 of a muon with initial energy E_0 is given by

$$x_0 \approx (1/b)\ln(1 + E_0/E_{\mu c})\ , \tag{23.29}$$

where $E_{\mu c} = a/b$. Figure 23.10 shows contributions to $b(E)$ for iron. Since $a(E) \approx 0.002$ GeV g^{-1} cm^2, $b(E)E$ dominates the energy loss above several hundred GeV, where $b(E)$ is nearly constant. The rate of energy loss for muons in hydrogen, uranium, and iron is shown in Fig. 23.11 [44].

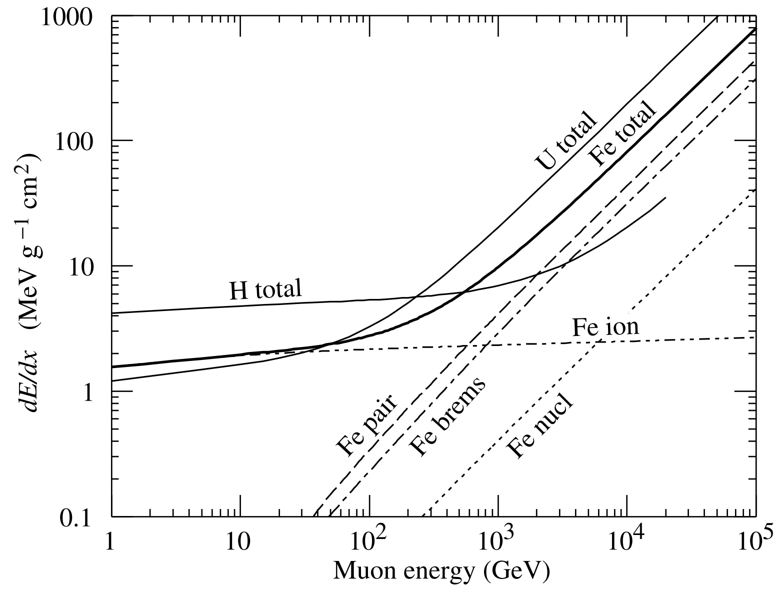

Figure 23.11: The average energy loss of a muon in hydrogen, iron, and uranium as a function of muon energy. Contributions to dE/dx in iron from ionization and the processes shown in Fig. 23.10 are also shown.

The "muon critical energy" $E_{\mu c}$ can be defined more exactly as the energy at which radiative and ionization losses are equal, and can be found by solving $E_{\mu c} = a(E_{\mu c})/b(E_{\mu c})$. This definition corresponds to the solid-line intersection in Fig. 23.6, and is different from the Rossi definition we used for electrons. It serves the same function: below $E_{\mu c}$ ionization losses dominate, and above $E_{\mu c}$ dominate. The dependence of $E_{\mu c}$ on atomic number Z is shown in Fig. 23.12.

The radiative cross sections are expressed as functions of the fractional energy loss ν. The bremsstrahlung cross section goes roughly as $1/\nu$ over most of the range, while for the pair production case the distribution goes as ν^{-3} to ν^{-2} (see Ref. 55). "Hard" losses are therefore more probable in bremsstrahlung, and in fact energy losses due to pair production may very nearly be treated as continuous. The calculated momentum distribution of an incident 1 TeV/c muon beam after it crosses 3 m of iron is shown in Fig. 23.13. The most probable loss is 9 GeV, or 3.8 MeV g^{-1}cm^2. The full width at half maximum is 7 GeV/c, or 0.7%. The radiative tail is almost entirely due to bremsstrahlung; this includes most of the 10% that lost more than 2.8% of their energy. Most of the 3.3% that lost more than 10% of their incident energy experienced photonuclear interactions, which are concentrated in rare, relatively hard collisions. The latter can exceed nominal detector resolution [56], necessitating the reconstruction of lost energy. Electromagnetic and hadronic cascades in detector materials can obscure muon tracks in detector planes and reduce tracking efficiency [57].

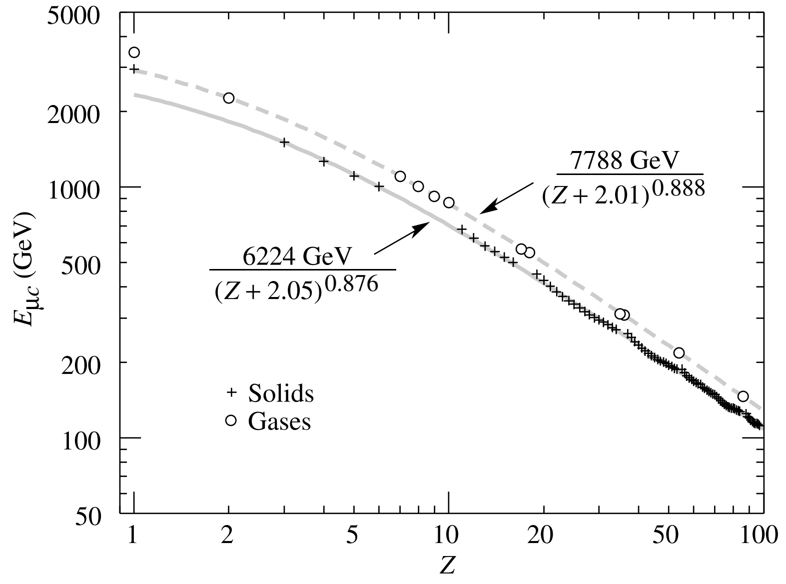

Figure 23.12: Muon critical energy for the chemical elements, defined as the energy at which radiative and ionization energy loss rates are equal. The equality comes at a higher energy for gases than for solids or liquids with the same atomic number because of a smaller density effect reduction of the ionization losses. The fits shown in the figure exclude hydrogen. Alkali metals fall 3–4% above the fitted function, while most other solids are within 2% of the function. Among the gases the worst fit is for neon (1.4% high). (Courtesy of N.V. Mokhov and S.I. Striganov.)

23.7. Čerenkov and transition radiation [4,58,59]

A charged particle radiates if its velocity is greater than the local phase velocity of light (Čerenkov radiation) or if it crosses suddenly from one medium to another with different optical properties (transition radiation). Neither process is important for energy loss, but both are used in high-energy physics detectors.

Čerenkov Radiation. The half-angle θ_c of the Čerenkov cone for a particle with velocity βc in a medium with index of refraction n is

$$\begin{aligned}\theta_c &= \arccos(1/n\beta) \\ &\approx \sqrt{2(1-1/n\beta)} \quad \text{for small } \theta_c, \textit{e.g.} \text{ in gases.}\end{aligned} \tag{23.30}$$

The threshold velocity β_t is $1/n$, and $\gamma_t = 1/(1-\beta_t^2)^{1/2}$. Therefore, $\beta_t\gamma_t = 1/(2\delta+\delta^2)^{1/2}$, where $\delta = n-1$. Values of δ for various commonly used gases are given as a function of pressure and wavelength in Ref. 60. For values at atmospheric pressure, see Table 6.1. Data for other commonly used materials are given in Ref. 61.

The number of photons produced per unit path length of a particle with charge ze and per unit energy interval of the photons is

$$\frac{d^2N}{dEdx} = \frac{\alpha z^2}{\hbar c}\sin^2\theta_c = \frac{\alpha^2 z^2}{r_e\, m_e c^2}\left(1 - \frac{1}{\beta^2 n^2(E)}\right)$$

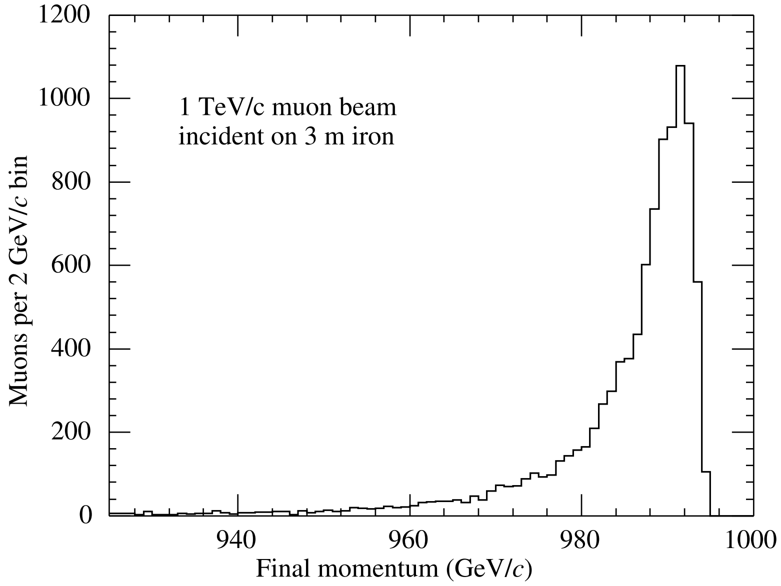

Figure 23.13: The momentum distribution of 1 TeV/c muons after traversing 3 m of iron, as obtained with Van Ginniken's TRAMU muon transport code [55].

$$\approx 370 \sin^2 \theta_c(E) \text{ eV}^{-1}\text{cm}^{-1} \qquad (z = 1) \,, \tag{23.31}$$

or, equivalently,

$$\frac{d^2N}{dx d\lambda} = \frac{2\pi\alpha z^2}{\lambda^2} \left(1 - \frac{1}{\beta^2 n^2(\lambda)}\right) \,. \tag{23.32}$$

The index of refraction is a function of photon energy E, as is the sensitivity of the transducer used to detect the light. For practical use, Eq. (23.31) must be multiplied by the the transducer response function and integrated over the region for which $\beta\, n(E) > 1$. Further details are given in the discussion of Čerenkov detectors in the Detectors section (Sec. 25 of this *Review*).

Transition Radiation. The energy radiated when a particle with charge ze crosses the boundary between vacuum and a medium with plasma frequency ω_p is

$$I = \alpha z^2 \gamma \hbar\omega_p/3 \,, \tag{23.33}$$

where

$$\begin{aligned} \hbar\omega_p &= \sqrt{4\pi N_e r_e^3}\; m_e c^2/\alpha \\ &= \sqrt{4\pi N_e a_\infty^3}\; 2 \times 13.6 \text{ eV} \,. \end{aligned} \tag{23.34}$$

Here N_e is the electron density in the medium, r_e is the classical electron radius, and a_∞ is the Bohr radius. For styrene and similar materials, $\sqrt{4\pi N_e a_\infty^3} \approx 0.8$, so that $\hbar\omega_p \approx 20$ eV. The typical emission angle is $1/\gamma$.

The radiation spectrum is logarithmically divergent at low energies and decreases rapidly for $\hbar\omega/\gamma\hbar\omega_p > 1$. About half the energy is emitted in the range $0.1 \leq \hbar\omega/\gamma\hbar\omega_p \leq 1$. For a particle with $\gamma = 10^3$, the radiated photons are in the soft x-ray range 2 to 20 eV. The γ dependence of the emitted energy thus comes from the hardening of the spectrum rather than from an increased quantum yield. For a typical radiated photon energy of $\gamma\hbar\omega_p/4$, the quantum yield is

$$\begin{aligned} N_\gamma &\approx \frac{1}{2}\,\frac{\alpha z^2\gamma\hbar\omega_p}{3}\Big/\frac{\gamma\hbar\omega_p}{4} \\ &\approx \tfrac{2}{3}\alpha z^2 \approx 0.5\% \times z^2\ . \end{aligned} \tag{23.35}$$

More precisely, the number of photons with energy $\hbar\omega > \hbar\omega_0$ is given by [4]

$$N_\gamma(\hbar\omega > \hbar\omega_0) = \frac{\alpha z^2}{\pi}\left[\left(\ln\frac{\gamma\hbar\omega_p}{\hbar\omega_0} - 1\right)^2 + \frac{\pi^2}{12}\right]\ , \tag{23.36}$$

within corrections of order $(\hbar\omega_0/\gamma\hbar\omega_p)^2$. The number of photons above a fixed energy $\hbar\omega_0 \ll \gamma\hbar\omega_p$ thus grows as $(\ln\gamma)^2$, but the number above a fixed fraction of $\gamma\hbar\omega_p$ (as in the example above) is constant. For example, for $\hbar\omega > \gamma\hbar\omega_p/10$, $N_\gamma = 2.519\,\alpha z^2/\pi = 0.59\% \times z^2$.

The yield can be increased by using a stack of plastic foils with gaps between. However, interference can be important, and the soft x rays are readily absorbed in the foils. The first problem can be overcome by choosing thicknesses and spacings large compared to the "formation length" $D = \gamma c/\omega_p$, which in practical situations is tens of μm. Other practical problems are discussed in Sec. 25.

References:

1. B. Rossi, *High Energy Particles*, Prentice-Hall, Inc., Englewood Cliffs, NJ, 1952.
2. U. Fano, Ann. Rev. Nucl. Sci. **13**, 1 (1963).
3. W.H. Barkas and M.J. Berger, *Tables of Energy Losses and Ranges of Heavy Charged Particles*, NASA-SP-3013 (1964).
4. J.D. Jackson, *Classical Electrodynamics*, 3rd edition, (John Wiley & Sons, New York, 1998).
5. "Stopping Powers and Ranges for Protons and Alpha Particles," ICRU Report No. 49 (1993).
6. J.D. Jackson, "Effect of Form Factor on dE/dx from Close Collisions," Particle Data Group Note PDG-93-04 (19 October 1993) (unpublished).
7. "Stopping Powers for Electrons and Positrons," ICRU Report No. 37 (1984).
8. `http://physics.nist.gov/PhysRefData/XrayMassCoef/tab1.html.`
9. S.M. Seltzer and M.J. Berger, Int. J. of Applied Rad. **33**, 1189 (1982).
10. S.M. Seltzer and M.J. Berger, Int. J. of Applied Rad. **35**, 665 (1984). This paper corrects and extends the results of Ref. 9.
11. R.M. Sternheimer, Phys. Rev. **88**, 851 (1952).
12. A. Crispin and G.N. Fowler, Rev. Mod. Phys. **42**, 290 (1970).

13. R.M. Sternheimer and R.F. Peierls, Phys. Rev. **B3**, 3681 (1971).
14. R.M. Sternheimer, S.M. Seltzer, and M.J. Berger, "The Density Effect for the Ionization Loss of Charged Particles in Various Substances," Atomic Data & Nucl. Data Tables **30**, 261 (1984). An error resulting from an incorrect chemical formula for lanthanum oxysulfide is corrected in a footnote in Ref. 10. Chemical composition for the tabulated materials is given in Ref. 9.
15. W.H. Barkas, W. Birnbaum, and F.M. Smith, Phys. Rev. **101**, 778 (1956).
16. M. Agnello *et al.*, Phys. Rev. Lett. **74**, 371 (1995).
17. H.H. Andersen and J.F. Ziegler, *Hydrogen: Stopping Powers and Ranges in All Elements.* Vol. 3 of *The Stopping and Ranges of Ions in Matter* (Pergamon Press 1977).
18. J. Lindhard, Kgl. Danske Videnskab. Selskab, Mat.-Fys. Medd. **28**, No. 8 (1954).
19. J. Lindhard, M. Scharff, and H.E. Schiøtt, Kgl. Danske Videnskab. Selskab, Mat.-Fys. Medd. **33**, No. 14 (1963).
20. J.F. Ziegler, J.F. Biersac, and U. Littmark, *The Stopping and Range of Ions in Solids*, Pergamon Press 1985.
21. L.D. Landau, J. Exp. Phys. (USSR) **8**, 201 (1944); See, for instance, K.A. Ispirian, A.T. Margarian, and A.M. Zverev, Nucl. Instrum. Methods **117**, 125 (1974).
22. W.R. Nelson, H. Hirayama, and D.W.O. Rogers, "The EGS4 Code System," SLAC-265, Stanford Linear Accelerator Center (Dec. 1985).
23. K. Hikasa *et al.*, *Review of Particle Properties*, Phys. Rev. **D46** (1992) S1.
24. For unit-charge projectiles, see E.A. Uehling, Ann. Rev. Nucl. Sci. **4**, 315 (1954). For highly charged projectiles, see J.A. Doggett and L.V. Spencer, Phys. Rev. **103**, 1597 (1956). A Lorentz transformation is needed to convert these center-of-mass data to knock-on energy spectra.
25. N.F. Mott and H.S.W. Massey, *The Theory of Atomic Collisions*, Oxford Press, London, 1965.
26. L.V. Spencer "Energy Dissipation by Fast Electrons," Nat'l Bureau of Standards Monograph No. 1 (1959).
27. "Average Energy Required to Produce an Ion Pair," ICRU Report No. 31 (1979).
28. N. Hadley *et al.*, "List of Poisoning Times for Materials," Lawrence Berkeley Lab Report TPC-LBL-79-8 (1981).
29. H.A. Bethe, Phys. Rev. **89**, 1256 (1953). A thorough review of multiple scattering is given by W.T. Scott, Rev. Mod. Phys. **35**, 231 (1963). However, the data of Shen *et al.*, (Phys. Rev. **D20**, 1584 (1979)) show that Bethe's simpler method of including atomic electron effects agrees better with experiment that does Scott's treatment. For a thorough discussion of simple formulae for single scatters and methods of compounding these into multiple-scattering formulae, see W.T. Scott, Rev. Mod. Phys. **35**, 231 (1963). For detailed summaries of formulae for computing single scatters, see J.W. Motz, H. Olsen, and H.W. Koch, Rev. Mod. Phys. **36**, 881 (1964).

30. V.L. Highland, Nucl. Instrum. Methods **129**, 497 (1975), and Nucl. Instrum. Methods **161**, 171 (1979).
31. G.R. Lynch and O.I Dahl, Nucl. Instrum. Methods **B58**, 6 (1991).
32. M. Wong *et al.*, Med. Phys. **17**, 163 (1990).
33. Y.S. Tsai, Rev. Mod. Phys. **46**, 815 (1974).
34. H. Davies, H.A. Bethe, and L.C. Maximon, Phys. Rev. **93**, 788 (1954).
35. O.I. Dahl, private communication.
36. M.J. Berger and S.M. Seltzer, "Tables of Energy Losses and Ranges of Electrons and Positrons," National Aeronautics and Space Administration Report NASA-SP-3012 (Washington DC 1964).
37. W.R. Nelson, T.M. Jenkins, R.C. McCall, and J.K. Cobb, Phys. Rev. **149**, 201 (1966).
38. G. Bathow *et al.*, Nucl. Phys. **B20**, 592 (1970).
39. *Experimental Techniques in High Energy Physics*, ed. by T. Ferbel (Addision-Wesley, Menlo Park CA 1987).
40. U. Amaldi, Phys. Scripta **23**, 409 (1981).
41. E. Longo and I. Sestili, Nucl. Instrum. Methods **128**, 283 (1975).
42. G. Grindhammer *et al.*, in *Proceedings of the Workshop on Calorimetry for the Supercollider*, Tuscaloosa, AL, March 13–17, 1989, edited by R. Donaldson and M.G.D. Gilchriese (World Scientific, Teaneck, NJ, 1989), p. 151.
43. P.H. Barrett, L.M. Bollinger, G. Cocconi, Y. Eisenberg, and K. Greisen, Rev. Mod. Phys. **24**, 133 (1952).
44. W. Lohmann, R. Kopp, and R. Voss, "Energy Loss of Muons in the Energy Range 1–10000 GeV," CERN Report 85–03 (1985).
45. H.A. Bethe and W. Heitler, *Proc. Roy. Soc.* **A146**, 83 (1934); H.A. Bethe, *Proc. Cambridge Phil. Soc.* **30**, 542 (1934).
46. A.A. Petrukhin and V.V. Shestakov, Can. J. Phys. **46**, S377 (1968).
47. V.M. Galitskii and S.R. Kel'ner, Sov. Phys. JETP **25**, 948 (1967).
48. S.R. Kel'ner and Yu.D. Kotov, Sov. J. Nucl. Phys. **7**, 237 (1968).
49. R.P. Kokoulin and A.A. Petrukhin, in *Proceedings of the International Conference on Cosmic Rays*, Hobart, Australia, August 16–25, 1971, Vol. **4**, p. 2436.
50. A.I. Nikishov, Sov. J. Nucl. Phys. **27**, 677 (1978).
51. Y.M. Andreev *et al.*, Phys. Atom. Nucl. **57**, 2066 (1994).
52. L.B. Bezrukov and E.V. Bugaev, Sov. J. Nucl. Phys. **33**, 635 (1981).
53. N.V. Mokhov, J.D. Cossairt, Nucl. Instrum. Methods **A244**, 349 (1986);
    N.V. Mokhov, Soviet J. Particles and Nuclei (Sept.–Oct. 1987) 408–426;
    N.V. Mokhov, "The MARS Code System User's Guide, Version 13(95)," Fermilab–FN–628, (April 1995).

54. L.B. Bezrukov and E.V. Bugaev, Sov. J. Nucl. Phys. **33**, 635 (1981).
55. A. Van Ginneken, Nucl. Instrum. Methods **A251**, 21 (1986).
56. U. Becker *et al.*, Nucl. Instrum. Methods **A253**, 15 (1986).
57. J.J. Eastman and S.C. Loken, in *Proceedings of the Workshop on Experiments, Detectors, and Experimental Areas for the Supercollider*, Berkeley, CA, July 7–17, 1987, edited by R. Donaldson and M.G.D. Gilchriese (World Scientific, Singapore, 1988), p. 542.
58. *Methods of Experimental Physics*, L.C.L. Yuan and C.-S. Wu, editors, Academic Press, 1961, Vol. 5A, p. 163.
59. W.W.M. Allison and P.R.S. Wright, "The Physics of Charged Particle Identification: dE/dx, Čerenkov Radiation, and Transition Radiation," p. 371 in *Experimental Techniques in High Energy Physics*, T. Ferbel, editor, (Addison-Wesley 1987).
60. E.R. Hayes, R.A. Schluter, and A. Tamosaitis, "Index and Dispersion of Some Čerenkov Counter Gases," ANL-6916 (1964).
61. T. Ypsilantis, "Particle Identification at Hadron Colliders", CERN-EP/89-150 (1989), or ECFA 89-124, **2** 661 (1989).